The Comparison with SAR Patterns of Biological Objects Contacted with Coaxial Waveguide Antenna Using the FDTD Method

S. M. Koo*, K. H. Kwon, C. W. Lee, C. H. Won, M. N. Kim**, and J. H. Cho
Department of Electronics, Kyungpook National University
*Department of Radio Communication, Doowon Technical College
**Dept. of Biomedical Engineering, Kyungpook National University Hospital

ABSTRACT

Noninvasive multifrequency microwave radiometry using coaxial waveguide antenna has been investigated for a homogeneous and four layer human body model. We derived finite-difference time-domain(FDTD) algorithm and equation of MUR and generalized perfectly matched layer(GPML) absorbing boundary conditions(ABCs) in cylindrical coordination. The coupling between coaxial waveguide antenna and a biological object was analyzed by use of the FDTD method using MUR and GPML ABCs to obtain the absorbed power patterns in the media. The specific absorption rates(SAR) distribution which was corresponding to the temperature distribution was calculated in each region by use of the steady-state response in FDTD method. The SAR patterns of FDTD method using MUR ABCs was compared with those of FDTD method using GPML ABCs.

I. Introduction

Noninvasive microwave radiometry has been investigated for temperature measurement in human body. With currently available technique, invasive thermometers are used in the clinic. In this method, number and positions of thermometer probes that can be inserted in the patent's body are quite limited by trauma considerations, resulting often in inadequate thermometry. Inserting and locating the thermometer probes are laborious and time consuming tasks for doctors, besides the probe insertion gives discomfort to the patient. For these reasons, development of noninvasive technique of temperature measurement has been desired and studied for many years.

Recently, the waveguide antenna has been used in experimental investigations of multifrequency microwave radiometry to develop noninvasive techniques of constructing temperature profiles and map in biological objects[1]. In these applications, the objects are lossy dielectric materials, such as a saline solution, phantom material, and a portion of human body. The portion of body coupled to the antenna is usually represented by a plane-parallel layered model consisting of, for example, the skin, fat and muscle. The problem of coupling between the rectangular waveguide antenna and the biological object of various configurations has been studied by a number of authors : Guy[2] and Katsumi[3]. Rectangular waveguide as an excitation source was contacted with the different models of the biological object in these studies. It is difficult to contact practical biological object with the rectangular waveguide in the clinical applications because it is too hard to bend and heavy.

In this paper, a new type of the noninvasive microwave radiometry which had no the above constraints was proposed and two models of human body were considered. One is the homogeneous model which is equivalent material with human muscle and the other is the four-layered model of human body. We derived FDTD algorithm and equation of MUR and GPML ABCs in cylindrical coordination. The coupling between coaxial waveguide antenna and two model medium was analyzed by use of the FDTD method using MUR and GPML ABCs to obtain the absorbed power pattern in the medium. The SAR distribution which was corresponding to the temperature distribution was calculated in each region by use of the steady-state response in FDTD method. The SAR patterns of FDTD method using MUR ABCs was compared with those of FDTD method using GPML ABCs. The comparison exhibits that the penetration depth of the SAR patterns using MUR ABCs is deeper than that of the SAR patterns using GPML ABCs because of loss in free space. However, the spread in the lateral directions of the SAR patterns using GPML ABCs is smaller than that of the SAR patterns using MUR ABCs.

II. Description of the problem

The geometry of the problem is shown in Fig. 1, along the coordinate system, where a coaxial waveguide antenna with a finite flange is radiating into a four-layered lossy medium. The relative dielectric constant of the coaxial waveguide is ε_r=76.4 and radii of inner and outer conductor are a=2.85mm and b=28.5mm, respectively.

In our present study, we treat a homogeneous lossy medium and a four-layered lossy medium. The homogeneous medium is a 0.4% saline solution at 30 ° C which is considered a muscle equivalent material.

The four-layered medium is assumed to consist of distilled-water(14.25mm), skin(1.9mm), fat(14.25mm) and muscle layer extending to infinity. Electrical properties of each material are listed in Table 1. Electrical properties of the saline solution and distilled-water(bolus) are obtained by Slogryan's equation[4], and those of the skin, fat and muscle are taken from Johnson and Guy[5].

The fundamental TEM mode is given at a plane normal to the waveguide axis which is 0.6λ away from coaxial end point as a source, as shown in Fig. 1, where λ is the wavelength in the coaxial waveguide. The incident electric field(source) E_ρ at the reference plane is given by

$$E_\rho^i(\rho,\ t) = \frac{\sin\omega t}{\ln(\frac{b}{a})\rho}, \tag{1}$$

where ω is the angular frequency.

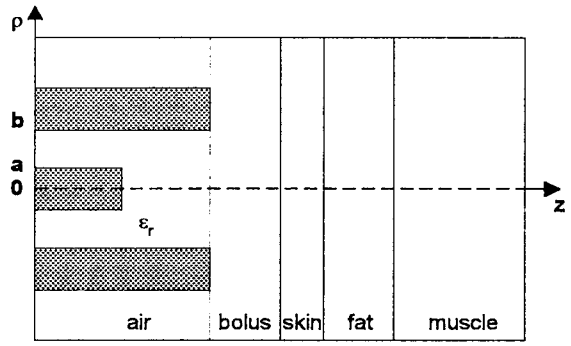

Fig. 1. Geometry of a coaxial antenna with a finite flange in contact with a 4-layered object.

Table 1. Electrical properties of biological materials used in this paper.

	dielectric constant(ε)	conductivity (σ : S/m)
0.4% saline solution(30 °C)	75.1	1.0
skin	49.7	1.7
fat	5.6	0.16
muscle	49.7	1.7
bolus (distilled-water)	76.4	0.26

In this paper, operating frequency is 1.2GHz. The FDTD method is used to calculate electromagnetic field in each region. Size of the cubic Yee cell is taken as Δ=0.95mm $\approx \lambda/30$s.

III. Yee's Algorithm

Yee[6] expressed Maxwell's curl equations in their finite-difference form. The Maxwell's curl equations used in the Yee/FDTD algorithm are

$$\nabla\times H = \frac{\partial D}{\partial t} + J,\quad \nabla\times E = -\frac{\partial B}{\partial t} \tag{2}$$

By expressing a continuous function of space and time in its discretized form, a function at its(nth) time step can be rewritten as

$$F^n(i,\ k) = F(i\Delta\rho,\ k\Delta z,\ n\Delta t) \tag{3}$$

After approximating the differential equations as difference equations and simplifying, following equations were obtained[7]

1. FDTD algorithm in the MUR boundary

$$\begin{aligned} H_\phi^{n+0.5}(i,k) &= H_\phi^{n-0.5}(i,k) \\ &+ \frac{\Delta t}{\mu_0\Delta\rho}[E_z^n(i+0.5,k) - E_z^n(i-0.5,k)] \\ &- \frac{\Delta t}{\mu_0\Delta z}[E_\rho^n(i,k+0.5) - E_\rho^n(i,k-0.5)] \end{aligned} \tag{4a}$$

$$\begin{aligned} E_\rho^{n+1}(i,k-0.5) &= \frac{1-\frac{\sigma(i,k-0.5)}{2\varepsilon(i,k-0.5)}}{1+\frac{\sigma(i,k-0.5)}{2\varepsilon(i,k-0.5)}} E_\rho^n(i,k-0.5) \\ &- \frac{\frac{\Delta t}{\varepsilon(i,k-0.5)\Delta z}}{1+\frac{\sigma(i,k-0.5)}{2\varepsilon(i,k-0.5)}} \\ &\times [H_\phi^{n+0.5}(i,k) - H_\phi^{n+0.5}(i,k-1)] \end{aligned} \tag{4b}$$

$$\begin{aligned} E_z^{n+1}(i+0.5,k) &= \frac{1-\frac{\sigma(i+0.5,k)}{2\varepsilon(i+0.5,k)}}{1+\frac{\sigma(i+0.5,k)}{2\varepsilon(i+0.5,k)}} E_z^n(i+0.5,k) \\ &- \frac{\frac{\Delta t}{\varepsilon(i+0.5,k)\rho(i+0.5,k)\Delta\rho}}{1+\frac{\sigma(i+0.5,k)}{2\varepsilon(i+0.5,k)}} \\ &\times [\rho(i+1,k)H_\phi^{n+0.5}(i+1,k) - \rho(i,k)H_\phi^{n+0.5}(i,k)] \end{aligned} \tag{4c}$$

where $\Delta\rho$, Δz are the space increments in ρ and z directions, respectively. Δt is time increment , c is the light velocity, σ is conductivity, ε is dielectric constant, μ_0 is permeability in free space and meet the stability criteria as set forth by Taflove[6] and given by

$$\Delta t \le \frac{1}{c}\sqrt{\frac{1}{\frac{1}{\Delta\rho^2}+\frac{1}{\Delta z^2}}} \tag{5}$$

2. FDTD algorithm in the GPML layer

$$\begin{aligned} H_\phi^{n+0.5}(i,k) &= H_\phi^{n-0.5}(i,k) \\ &+ \frac{\Delta t}{\mu\Delta\rho}[E_z^n(i+0.5,k) - E_z^n(i-0.5,k)] \\ &- \frac{\Delta t}{\mu\Delta z}[E_\rho^n(i,k+0.5) - E_\rho^n(i,k-0.5)] \end{aligned} \tag{6a}$$

$$\begin{aligned} E_\rho^{n+1}(i,k-0.5) &= \frac{2\varepsilon(i,k-0.5) - [\sigma_m(i,k-0.5) + \sigma_{gpml}(i,k-0.5)]\Delta t}{2\varepsilon(i,k-0.5) + [\sigma_m(i,k-0.5) + \sigma_{gpml}(i,k-0.5)]\Delta t} \\ &\times E_\rho^n(i,k-0.5) \\ &- \frac{2\sigma_m(i,k-0.5)\sigma_{gpml}(i,k-0.5)}{\mathrm{mod}\,1} \\ &\times (\Delta t)^2 \sum_{p=0}^{n} E_\rho^p(i,k-0.5) \end{aligned}$$

$$- \frac{1}{s(i,k)\Delta z} \times \frac{2\Delta t}{2\varepsilon(i,k-0.5)+[\sigma_m(i,k-0.5)+\sigma_{gpml}(i,k-0.5)]\Delta t} \times [H_\phi^{n+0.5}(i,k)-H_\phi^{n+0.5}(i,k-1)], \quad (6b)$$

$$\text{mod1} = 2\varepsilon^2(i,k-0.5)+\sigma(i,k-0.5) \times [\sigma_m(i,k-0.5)+\sigma_{gpml}(i,k-0.5)]\Delta t$$

$$E_z^{n+1}(i-0.5,k) = \frac{2\varepsilon(i-0.5,k)-[\sigma_m(i-0.5,k)+\sigma_{gpml}(i-0.5,k)]\Delta t}{2\varepsilon(i-0.5,k)+[\sigma_m(i-0.5,k)+\sigma_{gpml}(i-0.5,k)]\Delta t} \times E_z^n(i-0.5,k) - \frac{2\sigma_m(i-0.5,k)\sigma_{gpml}(i-0.5,k)(\Delta t)^2}{\text{mod2}} \times \sum_{p=0}^{n} E_z^p(i-0.5,k)$$

$$- \frac{1}{s(i,k)\rho(i-0.5,k)\Delta\rho} \times \frac{2\Delta t}{2\varepsilon(i-0.5,k)+[\sigma_m(i-0.5,k)+\sigma_{gpml}(i-0.5,k)]\Delta t} \times [\rho(i,k)H_\phi^{n+0.5}(i,k)-\rho(i-1,k)H_\phi^{n+0.5}(i-1,k)], \quad (6c)$$

$$\text{mod2} = 2\varepsilon^2(i-0.5,k)+\sigma(i-0.5,k) \times [\sigma_m(i-0.5,k)+\sigma_{gpml}(i-0.5,k)]\Delta t$$

where $\Delta\rho$, Δz are the space increments in ρ and z directions, respectively. Δt is time increment , c is the light velocity, $s(i,k)$ is a coefficient, σ_m is electric conductivity in the medium, and σ_{gpml} is electric conductivity in the GPML region.

IV. Absorbing boundary conditions

In order to model infinite space, boundary conditions at the computational lattice boundaries are needed. Since the computational lattice cannot be infinite for practical calculation, a finite region is used to model infinite space. When calculations stop at a fixed point in space, reflections occur at these computational boundaries. Lattice truncation conditions at the computation boundaries which simulate those of infinite space are therefore required. These absorbing boundary conditions absorb fields that are incident on the boundaries such that reflections do not occur. In our computation, the second-order ABCs based on Mur ABCs[8] and GPML ABCs[9] in the cylindrical coordinates are used on the truncation boundaries.

V. Simulation results

In this section, results of the FDTD computation at 1.2 GHz operating frequences are presented for two distinct cases:

(1) the antenna with the finite flange radiating into the homogeneous lossy medium,

(2) the antenna with the finite flange radiating into the four-layered medium.

The computation results are presented in the form of SAR distribution[10] that in given by following equation

$$SAR(i,k)=\frac{1}{2}\times\sigma(i,k)\times[E_\rho^2(i,k)+E_z^2(i,k)] \quad (7)$$

where E_ρ and E_z are computed from the positive and negative peak values in the FDTD analysis. SAR is proportiomal to temperature increment because it is energy absorption rates. Fig. 2 shows SAR distribution using MUR and GPML ABCs in the homogeneous lossy medium.

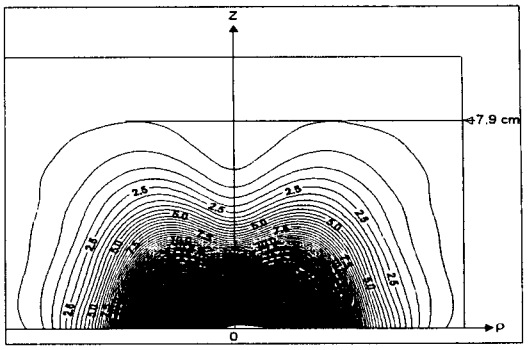

(a) using MUR ABCs

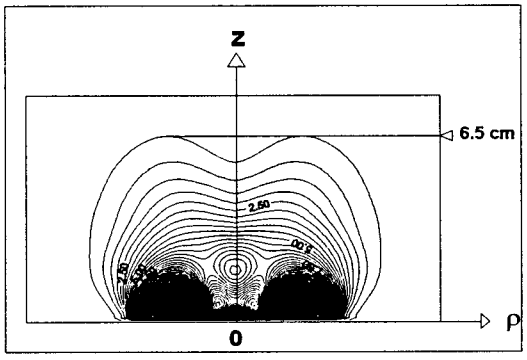

(b) using GPML ABCs

Fig. 2. SAR distribution in the homogeneous lossy medium for the antenna with the finite flange.

Fig. 3 shows SAR distribution using MUR and GPML ABCs in the four-layered medium. The pattern indicates that the SAR distributions spread out in the lateral directions, and the spreading is much larger than in the homogeneous medium. As consequence of the lateral spreading of the radiated power, the distance of power penetration along the z-axis is smaller in the 4-layered medium (using MUR ABCs : z=4.9 cm, using GPML ABCs: z=4.6 cm in Fig. 3) than in the homogeneous medum(using MUR ABCs: z=7.5 cm, using GPML ABCs: z=6.5 cm in Fig. 2). The SAR distribution in the 4-layered medium is affected very strongly by the presence of bolus and fat layers.

The lateral spreading of the electric fields in the 4-layered medium may be explained as following: a portion of the waves incident on the skin-fat and fat-muscle interfaces at oblique angles is reflected and trapped to excite waves propagating out in the lateral directons in the bolus and fat layer, and consequently in the skin layer as well. This phenomenon becomes stronger due to stronger diffraction by the antenna at lower operating frequencies.

The SAR patterns of FDTD method using MUR ABCs was compared with those of FDTD method using GPML ABCs. The comparison exhibits that the penetration depth of the SAR patterns using MUR ABCs is deeper than that of the SAR patterns using

GPML ABCs because of loss in free space. However, the spread in the lateral directions of the SAR patterns using GPML ABCs is smaller than that of the SAR patterns using MUR ABCs.

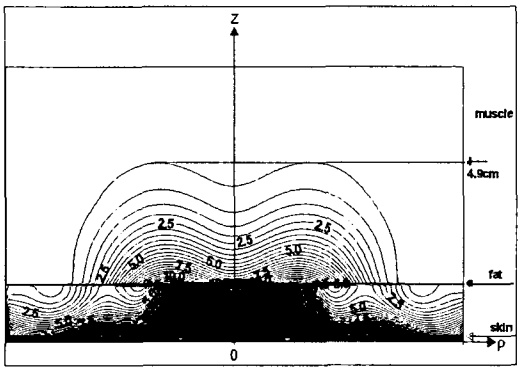

(a) using MUR ABCs

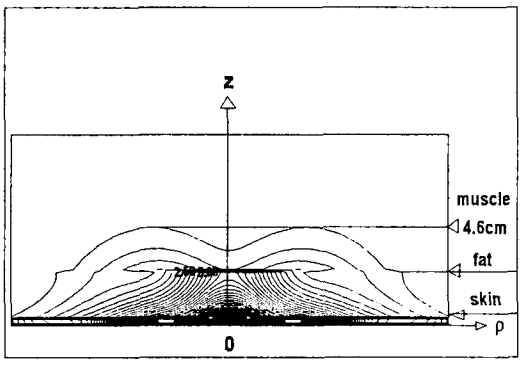

(b) using GPML ABCs

Fig. 3. SAR distribution in the four-layered medium for the antenna with the finite flange.

VI. Conclusion

The dielectric-filled coaxial waveguide antenna was designed for noninvasive hyperthermia application. We derived FDTD algorithm and equation of MUR and GPML ABCs in cylindrical coordination. The coupling between a dielectric-filled coaxial waveguide antenna and a four-layered biological medium was analyzed by use of the FDTD method. The second order MUR and GPML ABCs in the cylindrical coordinates was used on the truncation boundaries to model infinite space. The SAR patterns were calculated to predict the penetration depth of the electromagnetic field(or the temperature distribution) in the four-layered and homogeneous models of the human body. The simulation results indicate that SAR patterns tend to spread out in the lateral directions due to the presence of the bolus and the fat layer. The SAR patterns of FDTD method using MUR ABCs was compared with those of FDTD method using GPML ABCs. The comparison exhibits that the penetration depth of the SAR patterns using MUR ABCs is deeper than that of the SAR patterns using GPML ABCs because of loss in free space. However, the spread in the lateral directions of the SAR patterns using GPML ABCs is smaller than that of the SAR patterns using MUR ABCs. We are currently using the FDTD method to design a new type of coaxial waveguide antenna with proper flange dimensions to suppress the lateral spreading and to attain a deeper penetration depth of SAR distribution.

7. References

[1] S. Mizushina, T. Shimizu, K. Suzuki and T. Sugiura, "Retrival of temperature-depth profiles in biological objects from multifrequency microwave radiometric data," *J. of Electromagnetic Wave and Appl.*, Special issue on short-range sensing, pp. 1515-1548, 1993.

[2] A. W. Guy, "Electromagnetic fields and relative heating patterns due to a rectangular aperture source in direct contact with bilayered biological tissue," *IEEE Trans. Microwave Theory & Tech.*, vol. MTT-19, pp. 214-223, 1971.

[3] K. Abe, S. Mizoshiri, T. Sugiura and S. Mizushina, "Electromagnetic near fields of a rectangular waveguide antenna in contact with biological objects obtained by the FDTD method, " *IEICE Trans. Commun.*, vol. E78-B, no. 6, pp. 866-870, June 1995.

[4] S. Slogryan, "Equations for calculating the dielectric constant of saline water," *IEEE Trans. Microwave Theory & Tech.*, vol. MTT-19, pp. 733-736, 1971.

[5] C. C. Johnson and A. W. Guy, "Nonionizing electromagnetic wave effects in biological materals and systems," *Proc. IEEE*, vol. 60, pp. 692-718, 1972.

[6] A. Taflove and M. E. Brodwin, "Numerical solution of steady-state electromagnetic scattering problems using the time dependent Maxwell's equations," *IEEE Trans. Microwave Theory & Tech.*, vol. MTT-23, pp. 623-630, 1975.

[7] A. Taflove, *Computational Electrodynamics : The Finite-Difference Time-Domain Method*, Artech House, Boston, 1995.

[8] G. Mur, "Absorbing boundary conditions for the finite difference approximation of the time-domain electromagnetic field equations," *IEEE Trans. Electromag. Compat.*, vol. EMC-23, pp. 377-382, 1981.

[9] J. Fang and Z. Wu, "Generalized Perfectly Matched Layer-An Extension of Berenger's Perfectly Matched Layer Boundary Condition," *IEEE Microwave and Guided Letters.*, vol. 5, pp. 451-453, 1995.

[10] D. Sullivan, "Three-Dimensional Computer Simulation in Deep Regional Hyperthermia Using the FDTD Method," *IEEE Trans. Microwave Theory & Tech.*, vol. MTT-38, pp. 204-211, 1990.